Flow Cytometric Measurement of Cell Organelle Autophagy

N. Panchal, S. Chikte, B.R. Wilbourn, U.C. Meier and
G. Warnes

Additional information is available at the end of the chapter

1. Introduction

The term autophagy, (Type II Apoptosis) is derived from the Greek roots "auto" (self) and "phagy" (eat) and was first coined by De Duve in 1967 to epitomise this type of cell death. The mechanism of organelle autophagy in cells undergoing macro-autophagy (from here on termed autophagy) is poorly understood. Cytoplasm, misfolded protein aggregates, dysfunctional mitochondria and stressed endoplasmic reticulum (ER) are engulfed by the formation of a double membrane forming an autophagosome [1,2]. The formation of the autophagosome double membrane structure within the cytoplasm is thought to be formed from pre-existing membranes within the cell, although it is unknown whether the Golgi apparatus, endoplasmic reticulum (ER) or mitochondria are used preferentially to form the autophagosome structure [1,2]. During the formation of the autophagosome structure, organelles such as mitochondria, parts of the ER and Golgi apparatus are engulfed by the autophagosome with the final closure of the double membrane structure occurring next. This then fuses with nearby lysosomes, giving rise to an autolysosome, where the intracellular components are degraded by hydrolytic enzymes [1,3-5]. This process generates ATP, which may delay cell death if the cell is under nutrient depleted conditions leading to the survival of the cell. Thus it is unclear whether the process protects or causes diseases such as cancer and neurodegenerative disorders [6,7].

The process of autophagy is a cell survival mechanism that occurs when the cell is under stress, via external environmental pressures, including the lack of nutrients, or via the internal microenvironment of the cell, including the replacement of old and defective organelles such as mitochondria [8,9]. Autophagy is also induced by the formation and collection of misfolded proteins in the endoplasmic reticulum (ER) which causes ER-stress within the cell [10]. Prolonged adverse conditions results in the death of the cell by the autophagic process. The

ER is responsible for the folding and then delivery of proteins via the secretory pathway to a functional site. Misfolded proteins accumulate in the lumen of the ER due to high protein folding demand on the ER [10]. Only properly folded proteins are secreted with maintenance of the plasma membrane structure and ER folding capacity being under ER homeostatic control [10,11]. Once a threshold of misfolded protein accumulation has been reached, a signal activates the ER to nucleus signalling pathway or the Unfolded Protein Response (UPR) causing ER chaperone proteins to be synthesised which refold the misfolded proteins and translocate these proteins to the cytoplasm for degradation by the proteasome [10,11]. This process results in an increase of the ER capacity to fold proteins and maintain ER homeostasis. This increase in ER capacity is physically achieved by an increase in size of the ER at early stages of autophagy [12]. If the protein folding demand continues to increase, this will ultimately result in the phagy of the ER itself which can be caused by ER stress (induced *in vitro* by tunicamycin and dithiothreitol, (DTT) and also multiple mechanisms that induce autophagy *e.g.* drugs such as rapamycin and nutrient starvation [10].

Mitochondria are pivotal organelles in energy conversion. They act as the cell's power producers and are the site of cellular respiration, which ultimately generates fuel for the cell's activities. However, they are crucial for cell division, growth as well as cell death. As a major source of reactive oxygen species they consume cytosolic ATP when dysfunctional. It is, therefore pivotal for a cell to maintain of a cohort of healthy mitochondria. A sophisticated process called mitophagy, a selective process of autophagy, is responsible for the degradation of damaged organelles. In response to the triggers of mitophagy, mitochondria fragment, which sends out signals, which result in the engulfment by the autophagosomes [9,13]. Malfunctioning mitochondria are also generated through the process of aging or by having a high level of mutations in the mitochondrial DNA (mtDNA) induced by high levels of ROS. Mitochondrial DNA has 10-20 times more mutations than nuclear DNA [9]. Mitochondria reproduce by the process of fission, this produces two daughter mitochondria one of which hosts the damaged parts with reduced inner membrane potential of the original mitochondria but also a fully functional daughter [8]. The fission process can also stop excessive enlargement of mitochondria [8]. Conversely, mitochondrial fusion of damaged mitochondria dilutes the individual mitochondrion level of damaged macromolecules, and can prevent the early removal of such mitochondria [14]. Mitophagy is a physiological process which occurs during erythrocyte differentiation and during nutrient starvation [14]. The level of relative mitochondrial fusion and fission within cells maintains mitochondrial homoeostasis. Thus mitophagy provides a mechanism by which aged or ROS damaged mitochondria are ultimately removed resulting in the survival of the cell in question.

Different agents/stimuli induce autophagy via different signalling routes and thus may preferentially cause mitophagy or if the ER is stressed by such stimuli, ER phagy or ER enlargement may be detectable at specific time points during each treatment. To this end we have employed organelle mass dyes to measure the relative size of mitochondria and ER during nutrient starvation, rapamycin, and chloroquine treatments. We have previously developed and modified the technique employed by Ramdzan *et al* [15] to measure linear scaled fluorescent signals of MitoTracker Green and ER Tracker Green via a modification of

the cell cycle analysis doublet discrimination technique to accurately measure mitochondrial & ER mass during such treatments [16]. These techniques will serve as an adjunct to the measurement of autophagy microtubule associated protein, LC3I and LC3II (or LC3B as referred to from here on) in the determination of the presence of autophagy within a population of cells.

Methods for monitoring autophagy started with the initial discovery of the process by the use of electron microscopy showing the presence of double and single membrane structures termed the autophagosome and autolysosome or autophagolysosome respectively [4,5]. Other techniques have also obviously centred upon the formation of the autophagic machinery by measurement of LC3B, such as by Western Blotting which can be used to quantitate the degree of autophagy in cells by measuring LC3B which is normally located in the cytoplasm in the form of LC3I but when incorporated into the autophagosome is cleaved and lipidated by phosphotidylethanolamine, to form LC3II [17-19]. Anti-LC3B antibody labelling of LC3B has also been employed to measure autophagosomes and autolysosomes by image and flow cytometric analysis [20-22]. The increase in number and intensity of fluorescently labelled LC3B autophagosomes-autolysosomes can be quantitated by time-consuming image analysis, whereas increase in MFI of LC3B antigen levels measured flow cytometrically makes the process significantly less burdensome [21,23]. Here we describe a protocol to determine the presence of autophagy by the determination of LC3B levels in normal growing cells and those undergoing autophagy.

Use of techniques to estimate the degree of loss of dysfunctional cell organelles has been more limited than those techniques investigating the development of the autophagic process. Previous studies have used ER Tracker and MitoTracker mass probes from Invitrogen to estimate ER and mitochondrial size based on median fluorescence intensity [16]. In experimental conditions different inducers of autophagy such as rapamycin, chloroquine, serum and total nutrient starvation may result in the different types of cell organelles being preferentially targeted by the autophagic process. Here we describe quantitative flow cytometric methods, which can be employed in the study of cell organelle-phagy. We show that a range of inducers cause the phagy of specific organelles and that this process is also cell type dependent. This article will highlight ways of monitoring the contribution of distinctive cell organelles in vitro to the autophagic process and highlight its diversity in different cell types.

2. Materials and methods

2.1. Cell lines

Jurkat T and K562 cell lines were grown in RMPI-1640 with L-glutamine (Cat No 21875-034, Invitrogen, Paisley, UK) supplemented with 10% foetal bovine serum (FBS, Cat No 10500-064, Invitrogen, Paisley, UK) and penicillin and streptomycin (Cat No 15140-122, Invitrogen, Paisley, UK) in the presence of 5% CO_2 at 37°C.

2.2. Induction of autophagy

Jurkat and K562 cells were grown in <1% FBS-RPMI, <1% FBS-Phosphate Buffered Saline (PBS) (PBS, Cat No 14190-094 Invitrogen, Paisley, UK) or treated with chloroquine, (CQ) at 50μM, (Cat No C6628-25G, Sigma, Poole, UK), rapamycin (80nM, Cat No PHZ1233, Invitrogen, Paisley, UK). Time points analysed were 48h, (n=3) as described in the section below.

2.3. Indirect immunofluorescence LC3B labeling

Jurkat and K562 cells with or without treatment were pelleted and resuspended in 100 μl of Solution A fixative for 15 min at room temperature (RT) (Cat No GAS-002A-1, Caltag UK). Cells were then washed in PBS buffer Cell pellets were then permeabilised with 0.25% Triton X-100 (Cat No X100-500ML, Sigma Chemicals, Poole, UK) for 15 min at RT. Cells were washed in PBS buffer. Anti-LC3B polyclonal antibody (0.25 μg) (Cat No L10382, Invitrogen, Paisley, UK) or rabbit immunoglobulin (0.25 μg) (Cat No I5006, Sigma Chemicals, Poole, UK) was used as an isotype control and incubated for 0.5h at RT. Cells were then washed in PBS buffer. Cells were then labelled with 0.125 μg of secondary fluorescent conjugate Alexa Flour 647 goat anti-rabbit IgG (Cat No A21244, Invitrogen, Paisley, UK) for 30 min at RT. Cells were then washed in PBS buffer and resuspended in 400 μl of PBS. Analysis of LC3B-Alexa Fluor647 signal was achieved by determining the MFI of the whole histogram signal for previously gated cells from a FSC versus SSC dot-plot and compared to the corresponding isotype control sample in an overlaid histogram. 10,000 events were collected by flow cytometry.

2.4. Organelle labelling

Jurkat and K562 cells with or without treatment were counted and adjusted to the same number per volume and loaded with 40nM MitoTracker Green (MTG) (Cat No M7514, Invitrogen, Paisley, UK) or 100nM ER Tracker Green (ERTG) (Cat No L7526, Invitrogen, Paisley, UK) by incubating cells with dyes for 15 or 30 minutes at 37°C respectively. Cells were then washed in PBS buffer and resuspended in 400 μl of PBS, in the presence of DNA viability dye, DAPI (200 ng/ml) (Cat No D9542, Sigma Chemicals, Poole, UK). Live cells were analysed for MTG or ERTG MFI levels by firstly gating on all cell material except small debris in the origin of a FSC versus SSC dot-plot. This data was then analysed on a DAPI versus FSC dot-plot with live cells being DAPI-ve. The 530/30nm channel on a BD FACS Canto II was set to linear and the width parameter activated. Doublet discrimination was then achieved by gating on single cells on a 530/30nm width and area plot. Median fluorescence Intensity (MFI) of MTG-Area or ERTG-Area signals from samples was then compared by histogram analysis of untreated and treated cells.

2.5. Flow cytometry

Single colour controls for MTG, or ERTG and DAPI were used to set compensations. MTG or ERTG were detected in the 530/30nm channel on the argon laser octagon (BD FACSCanto II); DAPI was detected in the 440/40nm channel on the violet diode trigon (BD FACSCanto II). No

compensation was required. LC3B-Alexa Fluor-647 was detected on the 660/20nm channel on the Red HeNe trigon (BD FACSCanto II).

Cells (10,000) were analysed on a Becton Dickinson FACSCanto II fitted with a 488nm Ti-Sapphire Argon laser, red HeNe 633nm laser and violet diode 405nm with FACSDiva Software ver 6.1.3. All data were analysed on FlowJo (ver 8.8.7, Treestar Inc, CA) in the form of list-mode data files version FCS 3.00 using the default bi-exponential transformation. Optical filters and mirrors in the BD FACSCanto II were fitted in 2008.

2.6. Statistics

Student t tests were performed in Microsoft Office Excel with P = >0.05 not significant (NS), P = <0.05*, P = <0.01**, P = <0.005***, P = <0.001****.

3. Results

Cells treated to induce autophagy were first shown to be autophagic by immunofluorescent labelling of LC3B which is located in the autophagosome of cells undergoing autophagy. These were compared to resting control cells and positivity determine by use of an rabbit immuno-globulin isotype control labelled with the same secondary Alexa Fluor-647 conjugate permit-ting the demonstration that LC3B levels have been up-regulated in cell samples undergoing autophagy treatments. Figure 1 shows the LC3B signals from Jurkat and K562 cells after 48h of treatment compared to resting control levels. Resting cells do show a detectable LC3B compared to isotype controls (Figure 1). Jurkat cells showed a high level of LC3B compared to resting cells when treated with 80nM rapamycin and grown in low serum conditions (<1% FBS/RPMI, Figure 1A). In contrast CQ showed a lower level (half) of LC3B up-regulation compared to cells grown in nutrient free (<1% FBS) conditions (Figure 1B). K562 cell up-regulation of LC3B was shown to be at a similar level of that of Jurkat cells, when treated with rapamycin and grown in low serum conditions (<1% FBS/RPMI, Figure 1C). CQ and nutrient free (<1% FBS) treatment of K562 cells showed a similar LC3B response to that of Jurkat cells (Figure 1D).

Rapamycin was shown to significantly up-regulate LC3B by 4-5 fold after 24 and 48h (P=<0.001, P=<0.005) in both cell lines (Figure 2A, B). In contrast low serum conditions caused a 5-6 fold increase in Jurkat LC3B only at 48h (P=<0.001, Figure 2A). Whilst, K562 responded to low serum treatment by a lower but significant 2-3 fold increase in LC3B levels at 24 and 48h (P=<0.005, P=<0.05, Figure 2B). Likewise nutrient depletion of K562 cells caused a 2 fold increase in LC3B at 24 and 48h (P=<0.01, P=NS, Figure 2B). Whilst nutrient depletion of Jurkat cells showed a significant 5-6 fold increase at 24h, reduced to a significant 2 fold increase above controls at 48h (P=<0.005, Figure 2A). CQ (50μM) in contrast to rapamycin induced a 50-100% increase in LC3B levels in Jurkat cells at 24 and 48h respectively (P=<0.05, P=NS, Figure 2A). Whilst K562 cells responded to CQ treatment (50μM) by doubling LC3B levels at 24h and falling back to control levels at 48h respectively (P=NS, Figure 2B).
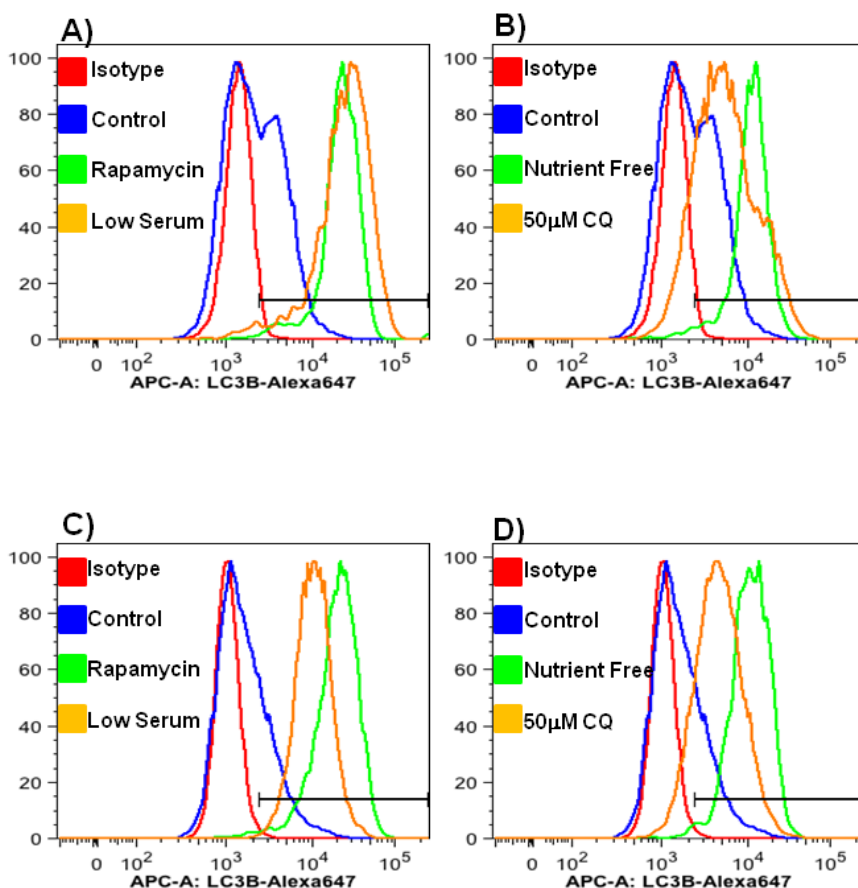
Figure 1. Demonstration of autophagy in Jurkat and K562 cells by measurement of LC3B levels by flow cytometry, see Materials & Methods. Resting Jurkat cell LC3B-Alexa Fluor-647 levels were compared after 48h treatment with 80nM rapamycin and low serum/RPMI LC3B levels A). Resting Jurkat cell LC3B-Alexa Fluor-647 levels were compared after 48h treatment of low serum/nutrient free conditions and CQ (50μM) LC3B levels B). Resting K562 cell LC3B-Alexa Fluor-647 levels were compared after 48h treatment with 80nM rapamycin and low serum/RPMI LC3B levels C). Resting K562 cell LC3B-Alexa Fluor-647 levels were compared after 48h treatment of low serum/nutrient free conditions and CQ (50μM) LC3B levels D).

Mitophagy was determined by linear flow cytometric analysis of the MTG signal in Jurkat and K562 cells by the following procedure. After gating on cells from a FSC v SSC dot-plot (Figure 3A), live cells were gated upon from a FSC v DAPI dot-plot (Figure 3B), DAPI negative cells being alive. Doublet discrimination was determined from an MTG Area v Width parameter plot (Figure 3C) and MFI of control and test samples compared on an overlaid histogram (Figure 3D). In this example the Jurkat cell control gave an MFI of 142,000 compared to a 50μM CQ test showing an MFI of 100,000 or a 30% reduction in the mitochondrial mass of live Jurkat cells.
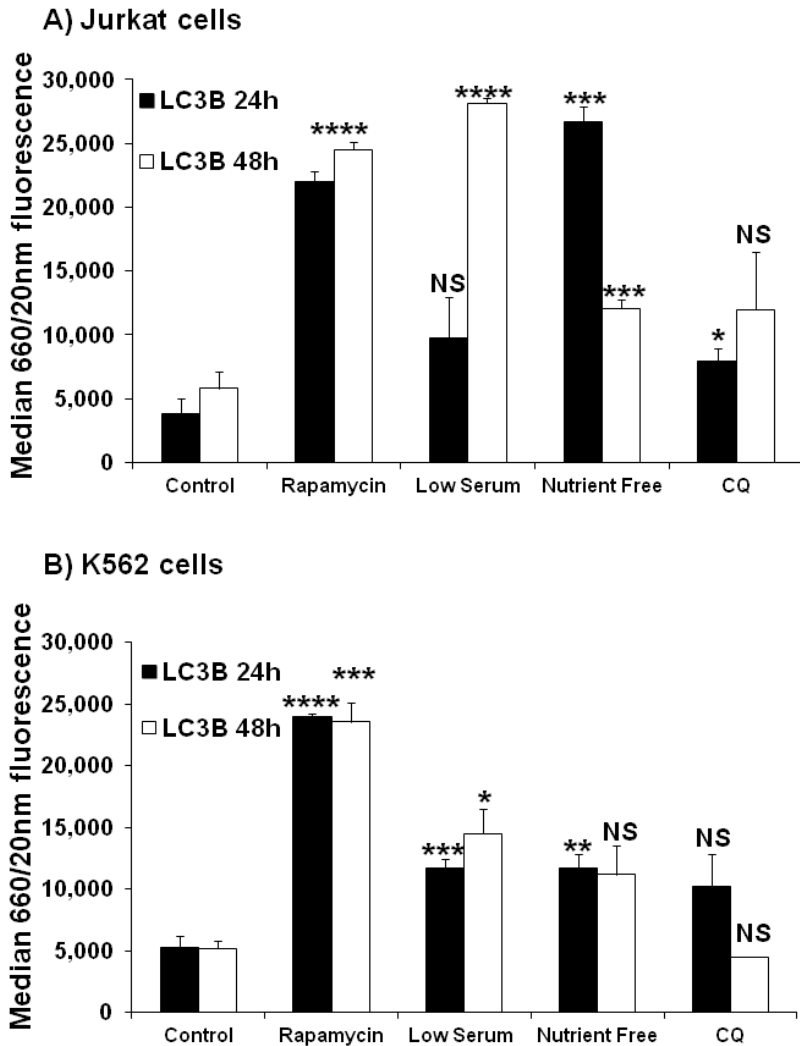
Figure 2. Demonstration of autophagy in Jurkat and K562 cells by measurement of MFI LC3B levels by flow cytometry, see Materials & Methods. Resting Jurkat cell MFI LC3B-Alexa Fluor-647 levels were compared after 24 and 48h treatment with 80nM rapamycin, low serum/RPMI, low serum/nutrient free conditions and CQ (50μM) LC3B levels A). Resting K562 cell MFI LC3B-Alexa Fluor-647 levels were compared after 24 and 48h treatment with 80nM rapamycin, low serum/RPMI, low serum/nutrient free conditions and CQ (50μM) LC3B levels A). T-test statistical analysis NS-not significant, * P=<0.05, ** P=<0.01, *** P=<0.005, **** P=<0.001.

Likewise ER-phagy was determined by linear flow cytometric analysis of the ERTG signal in Jurkat and K562 cells by the following procedure. After gating on cells from a FSC v SSC dot-plot (Figure 4A), live cells were gated upon from a FSC v DAPI dot-plot (Figure 4B), DAPI

negative cells being alive. Doublet discrimination was determined from an ERTG Area v Width parameter plot (Figure 4C) and MFI of control and test samples compared on an overlaid histogram (Figure 4D). In this example the K562 cell control gave an MFI of 159,000 compared to a 40nM rapamycin test showing an MFI of 262,000 or a 65% increase in the ER mass of live K562 cells.
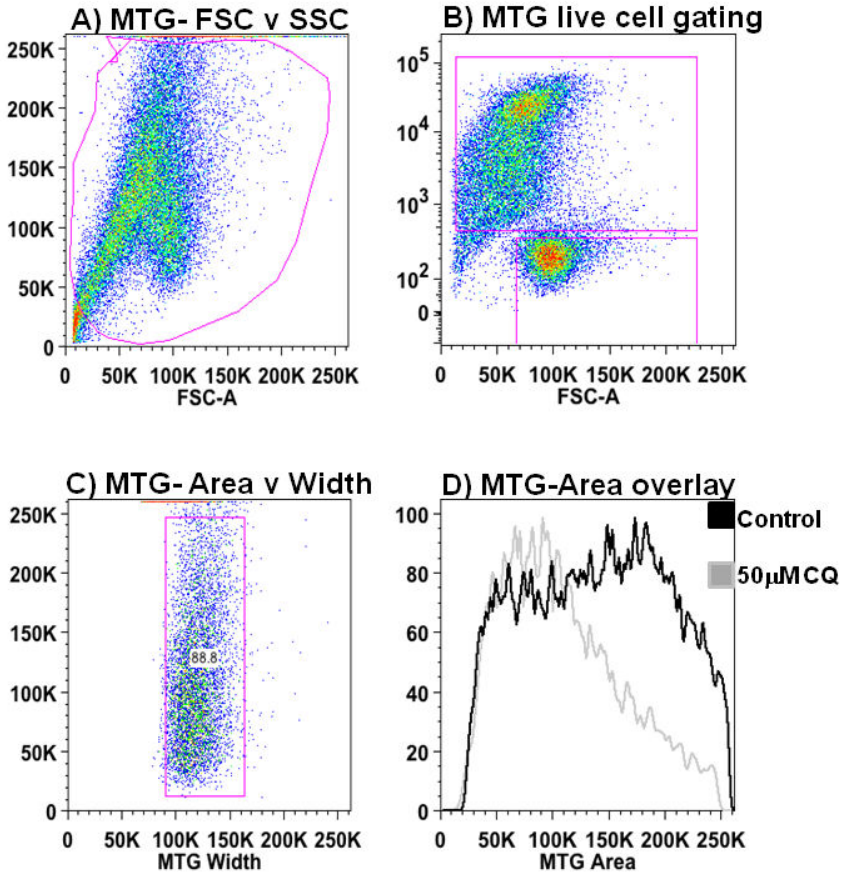

Figure 3. Jurkat cells were untreated (control) or treated with 50μM CQ for 48h. These cell cultures were then counted and adjusted to be the same number per volume and loaded with 40nM MTG for 15 minutes at 37°C. Cells were washed and adjusted to 0.5ml volume containing DAPI at 200ng/ml. Cells were then analysed on a BD Canto II according to Materials & Methods. Cells were gated upon except the small debris in the origin of a FSC versus SSC dot-plot (A). There data were then analysed on a DAPI versus FSC dot-plot with live cells being DAPI-ve (B). The 530/30nm channel on a BD FACS Canto II was set to linear and the width parameter activated. Doublet discrimination was then achieved by gating on single cells on a 530/30nm width and area plot (C). The MFI of MTG-Area signals from samples were then compared by histogram analysis of untreated, MFI 142,000 and CQ treated cells, MFI 100,000 (D).
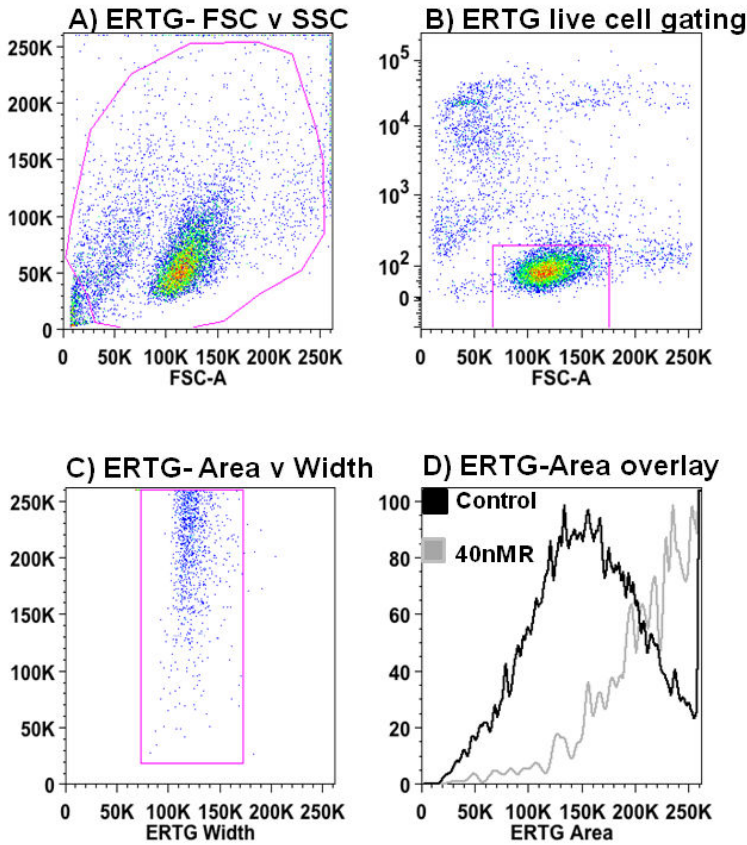
Figure 4. K562 cells were untreated (control) or treated with 40nM rapamycin (R) for 48h. These cell cultures were then counted and adjusted to be the same number per volume and loaded with 100nM ERTG for 30 minutes at 37°C. Cells were washed and adjusted to 0.5ml volume containing DAPI at 200ng/ml. Cells were then analysed on a BD Canto II according to Materials & Methods. Cells were gated upon except the small debris in the origin of a FSC versus SSC dot-plot (A). These data were then analysed on a DAPI versus FSC dot-plot with live cells being DAPI-ve (B). The 530/30nm channel on a BD FACS Canto II was set to linear and the width parameter activated. Doublet discrimination was then achieved by gating on single cells on a 530/30nm width and area plot (C). The MFI of ERTG-Area signals from samples were then compared by histogram analysis of untreated, MFI 159,000 and rapamycin treated cells, MFI 262,000 (D).

Induction of autophagy by the rapamycin mTOR signalling pathway induced a detectable mitophagy (34% reduction in mitochondrial mass) in Jurkat cells (Figure 5A). Whilst K562 cells displayed an ER stress response in that the ER mass was increased by 50% with rapamycin treatment without any mitophagy (Figure 5B). Like rapamycin, chloroquine induction of autophagy in Jurkat cells displayed a similar level of mitophagy (29%), whilst there was no significant organelle phagy displayed by K562 cells (Figure 5A, B). In contrast to rapamycin treatment of Jurkat cells, low serum/RPMI treatment caused a 19% increase in mitochondrial mass as opposed to a mitophagy. Under the same conditions Jurkat cells significantly increased

(37%, *P*<0.01) ER mass indicating a high level of misfolded proteins within the Jurkat cells (Figure 5A). However K562 cells responded in a similar manner to rapamycin treatment when treated with low serum/RPMI by displaying an increase in ER mass (43%) indicating again an autophagic response to a high level of misfolded proteins (Figure 5B). Nutrient depravation in the presence of low serum (<1%) showed the opposite response to low serum/RPMI treatment of cells in that a significant phagy of ER was observed in Jurkat cells (70%, *P*<0.05, Figure 5A). Whilst, K562 displayed both a significant ER phagy (42%) and mitophagy (36%), when undergoing nutrient depravation (*P*<0.05, Figure 5B).
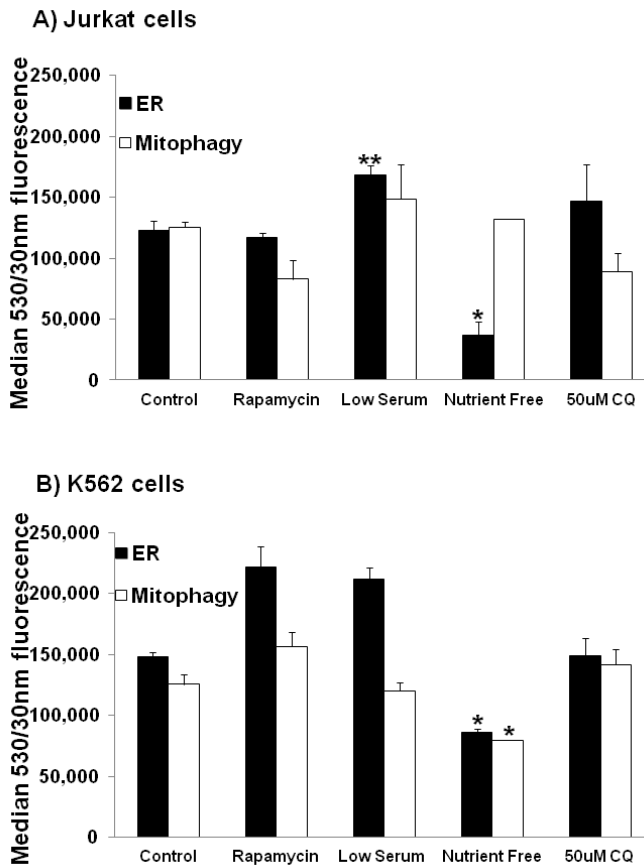

Figure 5. Jurkat (A) and K562 (B) cells were untreated (control) or treated 80nM rapamycin, low serum (<1% FBS) RPMI, nutrient free PBS (<1% FBS) or with 50μM CQ for 48h. These cell cultures were then counted and adjusted to be the same number per volume and loaded with 40nM MTG or 100nM ERTG for 15 or 30 minutes at 37°C respectively. Cells were washed and adjusted to 0.5ml volume containing DAPI at 200ng/ml. The MFI of MTG or ERTG-Area signals from samples were then compared by histogram analysis of untreated or treated cells. T-test statistical analysis NS-not significant, * P=<0.05, ** P=<0.01, *** P=<0.005, **** P=<0.001.

4. Discussion

Modulation of autophagy may be important in preventing or treating neurodegenerative conditions and cancers. It is, therefore, pivotal to understand the underlying mechanisms. Numerous new techniques have been developed to show that cells are undergoing the autophagic process; these include LC3B semi-quantification by image and flow cytometric analysis by the use of GFP tagged proteins or antibody labelling [17-22,24-30]. Here we demonstrate by flow cytometric measurement of anti-LC3B-Alexa Fluor-647 signals that rapamycin significantly up-regulated LC3B in Jurkat and K562 cells, whilst CQ at 50μM, induced in comparison a small degree of detectable up-regulated LC3B in both cell lines employed in this study. Nutrient depletion studies, including reduced serum <1% and lack of nutrients induced a low level of LC3B up-regulation in K562 cells compared to the high level (similar to rapamycin) detected in Jurkat cells.

Different drugs or treatments induce autophagy via different signalling routes in different cell types resulting in varying types and degrees of organelle phagy. Rapamycin although induced a similar LC3B up-regulation in the two cell lines employed in this study resulted in different organelle phagy responses. Jurkat cells showed a mitophagy whilst K562 cells did not. This was in contrast to the lack of an effect of rapamycin upon Jurkat ER mass, whilst K562 cells showed an increase in ER mass, indicating protein mis-folding within the ER, even though rapamycin caused little cell death over the 48h period studied [10,11]. This increase in ER size after 48h of rapamycin treatment may ultimately result in a measurable ER-phagy at a later time point.

Chloroquine induced apoptosis, death, low level autophagy (as indicated by mild LC3B up-regulation) and mitophagy as indicated by the reduction in mitochondrial mass in Jurkat cells, whilst no organelles were targeted in K562 cells [31]. Thus both rapamycin and chloroquine act upon Jurkat cells to produce a mitophagy with no significant affect upon ER mass; whilst K562 cell response to these autophagy inducers was to show an increase in ER mass.

Nutrient starvation commonly employed by removing serum from media in the study of autophagy caused protein mis-folding in both cell lines as indicated by an increase in ER mass and also of mitochondria in Jurkat cells [22]. In contrast total nutrient starvation which again caused varying degrees of up-regulation of LC3B levels in both cell lines as well as resulting in a large reduction in cell numbers caused a decrease in ER mass in both cell lines and a mitophagy in K562 cells. This again indicated that drug induction of autophagy may result in different organelle phagy in different cell types.

Thus the combination of measuring the induction of autophagy via LC3B flow cytometric measurements and the technique of organelle mass semi-quantification gives the investigator more information about the autophagic process occurring within the cell not only in terms of autophagic flux signals but also the degree and type of organelle phagy occurring during the autophagic process. This technique of organelle mass semi-quantification by flow cytometry on live cells permits researchers in the field to measure not only the degree of autophagy but also live cell functions such as mitochondrial membrane potential during the autophagic

process giving an insight to the more precise mechanism of action of the wide variety of stimuli that can be employed in the study of the autophagic process. This area warrants further study as it holds new therapeutic and diagnostic potential.

Author details

N. Panchal[1], S. Chikte[1], B.R. Wilbourn[1], U.C. Meier[2] and G. Warnes[1]

1 Flow Cytometry Core Facility, The Blizard Institute, Barts and The London School of Medicine and Dentistry, Queen Mary London University, UK

2 Centre for Neuroscience and Trauma, The Blizard Institute, Barts and The London School of Medicine and Dentistry, Queen Mary London University, London, UK

References

[1] Tooze S, Yoshimori T. The origin of the autophagosomal membrane. Nature Cell Biology 2010;12:831-835.

[2] Mehrpour M, Esclatine A, Beau I, Codogno P. Overview of macroautophagy regulation in mammalian cells. Cell Research 2010;20:748-762.

[3] Yang Z, Klionsky D. Eaten alive: a history of macroautophagy. Nature Cell Biology 2010;12:814-822.

[4] Ashford TP, Porter K. Cytoplasmic components in hepatic cell lysosomes. J Cell Biol 1962;12:198-202.

[5] Deter RL, Duve CD. Influence of glucagon, an inducer of cellular autophagy, on some physical properties of rat liver lysosomes. J Cell Biol 1967;33:437-449.

[6] Shintani T, Klionsky D. Autophagy in health and disease: A double-edged sword. Science 2004;306:990-995.

[7] Rosello A, Warnes G, Meier CU. Cell death pathways and autophagy in the central nervous system and its involvement in neurodegeneration, immunity and CNS infection: to die or not to die - that is the question. Clin Exp Imm 2012;168:52-57.

[8] Terman A, Gustafsson B, Brunk UT. Autophagy, organelles and ageing. The Journal of Pathology 2007;211:134-143.

[9] Kim I, Rodriguezenriquez S, Lemasters J. Selective degradation of mitochondria by mitophagy. Archives of Biochemistry and Biophysics 2007;462:245-253.

[10] Yorimitsu T, Klionsky DJ. Eating the endoplasmic reticulum: quality control by autophagy. Trends in Cell Biology 2007;17:279-285.

[11] Mandl J, Mészáros T, Bánhegyi G, Hunyady L, Csala M. Endoplasmic reticulum: nutrient sensor in physiology and pathology. Trends in Endocrinology & Metabolism 2009;20:194-201.

[12] Bernales S, McDonald KL, Walter P. Autophagy counterbalances endoplasmic reticulum expansion during the unfolded protein response. PLoS Biology 2006;4:e423.

[13] Kanki T, Klionsky DJ. The molecular mechanism of mitochondria autophagy in yeast. Molecular Microbiology 2010;75:795-800.

[14] Twig G, Shirihai OS. The interplay between mitochondrial dynamics and mitophagy. Antioxidants & Redox Signaling 2011;14:1939-1951.

[15] Ramdzan YM, Polling S, Chia CPZ, Ng IHW, Ormsby AR, Croft NP, Purcell AW, Bogoyevitch MA, Ng DCH, Gleeson PA and others. Tracking protein aggregation and mislocalization in cells with flow cytometry. Nat Meth 2012;9:467-470.

[16] Jia W, He YW. Temporal regulation of intraclualr organelle homeostasis in T lymphocytes by autophagy. The Journal of Immunology 2011;186:5313-5322.

[17] Kabeya Y, Mizushima N, Ueno T, Yamamoto A, Kirisako T, Noda T, Kominami E, Ohsumi Y, T. Y. LC3, a mammalian homologue of yeast Apg8p, is localized in autophagosome membranes after processing. EMBO 2000;19:5720-5728.

[18] Barth S, Glick D, Macleod K. Autophagy: assays and artifacts. The Journal of Pathology 2010;221:117-124.

[19] Hansen TE, Johansen T. Following autophagy step by step. BMC Biology 2011;9:1-4.

[20] Geng Y, Kohil L, Klocke BJ, Roth KA. Chloroquine-induced autophagic vacuole accumulation and cell death in glioma cells is p53 independent. Neuro-Oncology 2010;12:473-481.

[21] Thomas S, Thurn KT, Biçaku E, Marchion DC, Münster N. Addition of a histone deacetylase inhibitor redirects tamoxifen-treated breast cancer cells into apoptosis, which is opposed by the induction of autophagy. Breast Cancer Research and Treatment 2011;130:437-447.

[22] Phadwal K, Alegre-Abarrategui J, Watson AS, Pike L, Anbalagan S, Hammond EM, Wade-Martins R, McMichael A, Klenerman P, Simon AK. A novel method for autophagy detection in primary cells: Impaired levels of macroautophagy in immunosenescent T cells. Autophagy 2012;8:677-689.

[23] Chen Y, McMillan-Ward E, Kong J, Israels SJ, Gibson S. Oxidative stress induces autophagic cell death independent of apoptosis in transformed and cancer cells. Cell Death and Differentiation 2007;15:171-182.

[24] Shvets E, Fass E, Elazar Z. Utlizing flow cytometry to monitor autophagy in living mammalian cells. Autophagy 2008;4:621-628.

[25] Kimura S, Noda T, Yoshimori T. Dissection of the autophagosome maturation process by a novel reporter protein, tandem fluorescent-tagged LC3. Autophagy 2007;3:452-460.

[26] Wu YT, Tan HL, Huang Q, Kim YS, Pan N, Ong WY, Liu ZG, Ong CN, Shen HM. Autophagy plays a protective role during zVAD-induced necrotic cell death. Autophagy 2008;4:457-466.

[27] Boya P, Gonzalez-Polo RA, Poncet D, Andreau K, Vieira HLA, Roumier T, Perfettini JL, Kroemer G. Mitochondrial membrane permeabilization is a critical step of lysosome-initiated apoptosis induced by hydroxychloroquine. Oncogene 2003;22:3927-3936.

[28] Boya P, Gonzalez-Polo RA, Casares N, Perfettini JL, Dessen P, Larochette N, Metivier D, Meley D, Souquere S, Yoshimori T and others. Inhibition of macroautophagy triggers apoptosis. Molecular and Cellular Biology 2005;25:1025-1040.

[29] Byun JY, Yoon CH, An S, Park IC, Kang CM, Kim MJ, SJ. L. The Rac1/MKK7/JNK pathway signals upregulation of Atg5 and subsequent autophagic cell death in response to oncogenic Ras. Carcinogenesis 2009;30:1880-1888.

[30] Mellen MA, dela Rosa EJ, Boya P. Autophagy is not universally required for phosphatidyl-serine exposure and apoptotic cell engulfment during neural development. Autophagy 2009;5:964-972.

[31] Cao C, Subhawong T, Albert JM, Kim KW, Geng L, Sekhar KR, Gi YJ, B. L. Inhibition of mammalian target of rapamycin or apoptotic pathway induces autophagy and radiosensitizes PTEN null prostate cancer cells. Cancer Research 2006;66:10040-10047.